Environmental Science
Water Research & Technology

Long-Term Surveillance of Wastewater SARS-CoV-2 in Los Angeles County

Journal:	*Environmental Science: Water Research & Technology*
Manuscript ID	EW-ART-08-2021-000586.R1
Article Type:	Paper

Water Impact Statement

We demonstrate wastewater-based epidemiology (WBE) as an effective tool to monitor communal viral load of SARS-CoV-2 over multiple infection outbreaks in Los Angeles County. When paired with clinical data, WBE could help identify communities requiring increased in-person testing. Further, WBE data can be used to estimate the number of infected individuals to better understand community disease impact.

Long-Term Surveillance of Wastewater SARS-CoV-2 in Los Angeles County

Phillip Wang[a], Ali Zarei-Baygi[a], Connor Sauceda[a], Syeed Md Iskander[b], Adam L. Smith[a]*

[a] Sonny Astani Department of Civil and Environmental Engineering, University of Southern California, 3620 South Vermont Avenue, Los Angeles, California 90089, United States

[b] Department of Civil, Construction and Environmental Engineering, North Dakota State University, Fargo, ND 58102, USA

*Corresponding author

Abstract

Wastewater-based epidemiology (WBE) is an effective and versatile tool for monitoring communal viral load. In addition, WBE can enhance clinical surveillance by identifying potential under testing communities. Here we report the results of WBE surveillance of Los Angeles County, CA, one of the largest and most populated metropolises in the United States. We collected weekly samples of 24-hour flow-weighted composite influent from five wastewater treatment plants for 44 weeks. Wastewater SARS-CoV-2 levels were quantified using RT-qPCR targeting the CDC recommended nucleocapsid genes N1 and N2. During our study, wastewater SARS-CoV-2 levels in Los Angeles County experienced two large spikes, once during July-August 2020 and a second during December 2020-January 2021. Wastewater SARS-CoV-2 levels peaked at 3.85E+05 N1 gene copies/L and 3.79E+05 N2 gene copies/L during the first spike and 2.55E+06 N1 gene copies/L and 2.15E+06 N2 gene copies/L during the second spike. Pearson correlation analysis of wastewater SARS-CoV-2 levels with clinical data showed strong correlations of $r = 0.94$, $p << 0.01$ for N1 and N2. Further, wastewater SARS-CoV-2 levels from samples collected once a day, over the course of a week, led clinical data by up to 5 days, which suggests WBE could be used as an early warning system for rising community infections. Monte Carlo simulations, using our measured wastewater SARS-CoV-2 dataset, estimated the number of infected individuals peaked on January 19th, 2021 with about 1.25 million active cases. The estimated total number of infected individuals for the duration of this study was 3.42 million people, which represents 34.2% of the population residing in Los Angeles County. Interestingly, our estimated number exceeds the cumulative clinical case count by almost 2 million people. This study demonstrates the utility of WBE to track infection dynamics within large communities. Further, WBE data can be used in Monte Carlo simulations to estimate the size of the infected population and complement clinical data-based models to better understand the disease impact on different communities.

Introduction

With the rapid and extensive spread of coronavirus disease 2019 (Covid-19) across the United States, large-scale monitoring tools, such as wastewater-based epidemiology (WBE), are gaining interest as a potential solution to help identify and track the spread of the virus, severe acute respiratory syndrome coronavirus 2 (SARS-CoV-2). WBE is an attractive candidate for communal monitoring of SARS-CoV-2 as it offers public health systems an economical, non-invasive, and readily deployable tool that complements in-person clinical nasal/saliva testing(1,2). While in-person testing provides invaluable diagnostic power to understand the size and demographic of the infected population, issues with potential sampling bias, reporting delays, and costs are exacerbated when the capacity to provide in-person testing is limited. WBE offers many advantages that mitigate the shortcomings of in-person testing. For example, wastewater samples are taken from communal waste streams that draws from all contributing individuals with equal probability and therefore avoids the potential sampling bias and inconvenience stemming from the opt-in nature of in-person testing. Further, WBE requires a relatively short turn-around time, with a number of workflows offering samples to results in under six hours, regardless of community size, versus one to three days for clinical nasal/saliva tests(3). With faster time to results, WBE can identify outbreaks or emerging hotspots in near real-time. Wastewater samples can be used in a variety of assays such as RT-qPCR to quantify biomarkers for SARS-CoV-2 (e.g., nucleocapsid genes N1 and N2) and metagenomic sequencing to assess variant composition. In the wake of evolving SARS-CoV-2 variants, RT-qPCR and metagenomic sequencing may be used on stored or fresh wastewater samples to assess the SARS-CoV-2 variant composition in specific communities over time(4,5).

To date, SARS-CoV-2 has been detected in wastewater from countries around the world including, but not limited to, Turkey(6), Germany(7), Netherlands(8), Australia(9), Japan(10), and the United States(11). While previous WBE studies have demonstrated that trends in regional clinical cases of Covid-19 are reflected in wastewater(12), attempts to back-calculate the infected population size from wastewater SARS-CoV-2 data face multi-faceted and complex uncertainties stemming from inconsistent viral loading and system-specific factors of each wastewater collection system. For instance, while studies estimate around 48% of the SARS-CoV-2 infected population shed detectable levels of the virus in their stool(13), reports of SARS-CoV-2 in stool samples range between 10^2 -10^8 virus copies/gram of feces. Further, estimates place the viral shedding period range between 1-33 days, and in rare cases up to 47 days(12,13). Apart from viral loading, the impact of system-specific factors (e.g., combined or separate collection systems, wastewater strength, sewer travel time, and temperature) on the detection and interpretation of the data remains an area needing further refinement(14). For a detailed assessment of the various variables and uncertainties in back-calculating infected population size with measured wastewater SARS-CoV-2 data please refer to the review on this topic by Li et al., 2021(15).

In this study, we showcase the utility of WBE by monitoring wastewater SARS-CoV-2 load from five wastewater treatment plants (WWTPs) in Los Angeles County, CA over the course of 44 weeks. The five WWTPs sampled in this study vary in size, with an average influent flow rate

between 9.87 to 941 million liters per day (MLD) and service populations between 150,000 to 4,000,000 residents each. Collectively, the sampled WWTPs serve over 9 million people, which accounts for more than 90% of the population in Los Angeles County. More notably, Los Angeles County experienced the highest prevalence of new Covid-19 cases of all US cities during the winter surge (November-January), with 27,906 new cases per day at its peak. Wastewater SARS-CoV-2 load was quantified using the CDC recommended N1 and N2 gene targets within the SARS-CoV-2 genome via RT-qPCR. Wastewater SARS-CoV-2 data along with parameters for stool load, viral load, and percentage of infected population for viral shedding were used to estimate the number of infected individuals via Monte Carlo simulations. System-specific factors (SSF) for each of the sampled WWTPs were explored for possible influencing variables that may improve the implementation of large-scale WBE efforts.

Materials and Methods

Sample Collection and Enveloped Virus Concentration

Twenty four-hour flow-weighted composite influent samples were collected from each WWTP on a weekly basis starting from May 12th, 2020 to March 10th, 2021 (Figure 1, Table 1), except for Joint Water Pollution Control Plant which was collected twice per week. All samples were kept on ice during transport from the collection site to the lab and immediately heat treated at 60°C for 90 min to inactivate the SARS-CoV-2 virus. Samples were concentrated in duplicates, where one replicate underwent RNA extraction, and the second replicate was stored at -80°C. The second replicate was processed when reverse transcription or qPCR inhibition was detected during RT-qPCR runs. A total sample volume of 50 mL was transferred from each sample into respective sterile 50 mL falcon tubes (Thermo Fisher Scientific, PA). An adsorption and elution method was used to concentrate the SARS-CoV-2 virus in each 50 mL sample(16,17). Briefly, each 50 mL sample was conditioned to an approximate 25 mM $MgCl_2$ final concentration. Conditioned samples were filtered through a 0.45 um HA membrane filter (Whatman) using a 250 mL vacuum filtration setup (Sterlitech, WA). HA filters trap enveloped viruses based on charge repulsion.

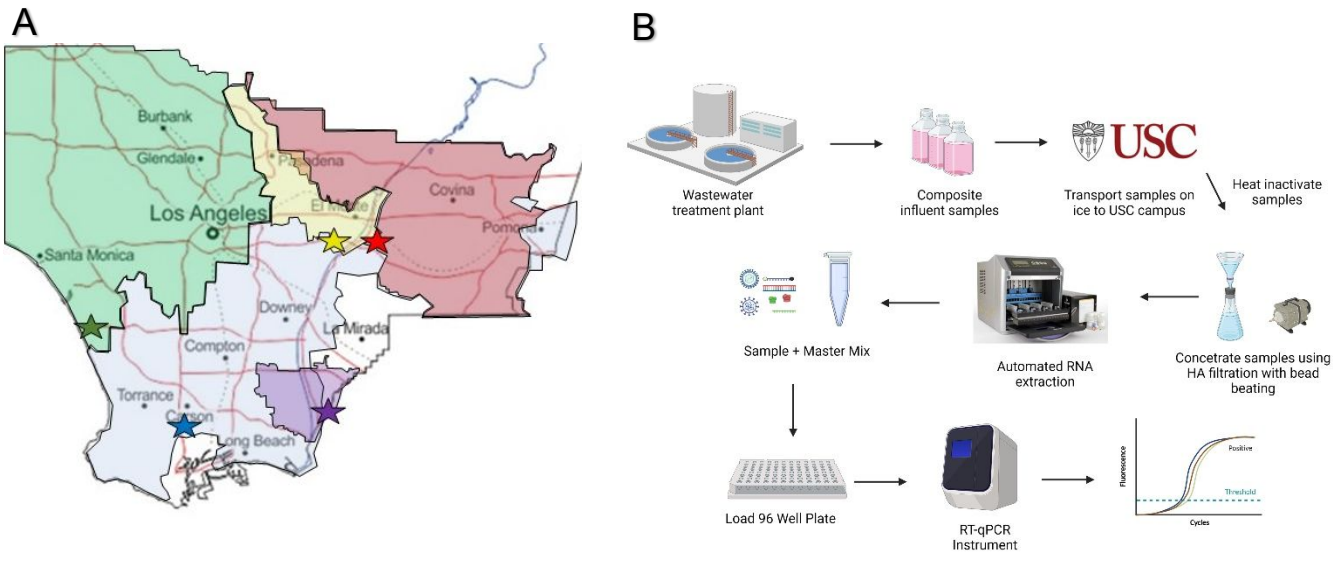

Figure 1A-B: 1A) Map of LA county and sampled sewersheds. Stars represent approximate location of each sampled WWTP. Orange = Hyperion, Blue = Joint Water Pollution Control Plant, Purple= Long Beach Water Reclamation Plant, Red = San Jose Creek Water Reclamation Plant, and Yellow = Whittier Narrows Water Reclamation Plant. 1B) Diagram of the general workflow used in this study to concentrate and measure wastewater SARS-CoV-2

.

Table 1: Collections Sites, Flow Rate, People Served, and Sample Frequency. Composite influent samples

Utility	Average Flow Rate (MLD)	Population Serviced	Frequency (per week)
Hyperion (HYP)	941	4,000,000	1
San Jose Creek (SJ)	36.8	992,000	1
Joint Water (JW)	305	3,500,000	2
Whittier Narrows (WN)	9.87	150,000	1
Long Beach (LB)	16.5	250,000	1

RNA Extraction

Total RNA was extracted from processed HA membrane filters using zirconium bead beating and the Maxwell 16 LEV simply RNA, blood purification kit (Promega, Madison WI) according to the manufacturer's instructions. HA filtration was chosen as the virus concentration method based on its ease of use, low cost, and consistent high recovery of gene targets compared to other widely used virus concentration methods(18). Preliminary assessment of our process workflow efficiency, using spiked bovine coronavirus (BCoV) seeded in heat-inactivated wastewater samples, achieved an extraction efficiency of 64.7% ± 1.86% (n=3), which is comparable to the 65.7% ± 23% recovery efficiency reported by Ahmed et al. using murine hepatitis virus(17). Similarly, our results are comparable to the recovery efficiency reported for HA filtration studies using BCoV as the proxy virus which range between 27.3-60.5% ± 22.2% (18,19). Although many studies use a proxy virus of known titer in each sample to adjust the measured SARS-CoV-2 data, we feared adjusting our measured wastewater SARS-CoV-2 data with the recovery efficiency of a proxy virus may introduce more biases than it corrects for(20). Therefore, we here report all SARS-CoV-2 data in its unadjusted form

SARS-CoV-2 Quantification

RNA extracts were analyzed using the SARS-CoV-2 RT-qPCR detection kit (Promega, Madison, WI). Each reaction consisted of 2.5 µL of RNA extract, 5 µL of 2x Go Taq Wastewater Master Mix, 0.5 µL of 20X Prime/Probe/Internal Amplification Control Mix, 0.2 µL, GoScript Reverse Transcriptase (50X), and 1.8 µL of nuclease free water, for a total final reaction volume of 10 µL. Each RT-qPCR reaction is designed to be a triplex assay targeting either the N1 or N2 gene (Hex), Pepper Mild Mottle Virus (reverse transcription inhibition control, FAM), and an internal DNA template (qPCR inhibition control, Cy5). All RT-qPCR reactions were done in triplicates and carried out using the LightCycler 96 instrument (Roche). All RT-qPCR runs included a a no template control, where 3 µL nuclease free water were used in place of the RNA extract and an RNA positive control containing the N and E genes (Promega, Madison WI). Only RT-qPCR runs with non-detects in the no template control were used for downstream analysis. Standard curves were generated by analyzing five ten-fold serial dilutions of the manufacturer provided linear dsDNA template ($1x10^5$–$1x10^1$ gene copies/reaction), which contains partial fragments of the N1, N2, and E gene. Please refer to SI Table 2 for a complete list of names and concentrations of the primes and probes used for the RT-qPCR assay. The thermocycling condition for all RT-qPCR runs were 1 cycle at 42°C for 15 min and 95°C for 2 min, followed by 40 cycles at 95 °C for 3 sec and 62°C for 30 seconds. Cq values above 40 were considered invalid and not used for downstream analysis. Only data within the acceptable Cq range for each inhibition control and a qPCR reaction efficiency value greater than or equal to 90% were used for downstream analysis. RT-qPCR reaction efficiencies were generated by the software provided with the LightCycler instrument (Roche)The SARS-CoV-2 copy number in gene copies per L for each wastewater sample was calculated using the RT-qPCR data for N1 and N2 multiplied by the concentration factor used in this study. The concentration factor was determined based on equation 1.

$$\frac{(\boldsymbol{Elution\ Volume})}{(\boldsymbol{Analyzed\ Volume})} \times \frac{(\mathbf{1{,}000\ \boldsymbol{mL}})}{(\boldsymbol{Sample\ Volume})} = \boldsymbol{Concentration\ Factor}\ \ (\mathbf{1})$$

Limit of detection for our RT-qPCR assay was assessed using the manufacturer provided RNA template, which encodes the N and E genes. A set of ten-fold serial dilutions were prepared from $1x10^5$–$1x10^0$ gene copies/reaction and mixed with the reaction mix as previously described. The limit of detection was called when only 60% (3 out of 5) of the prepared concentration successfully amplified.

Process flow and inhibition control assessment

Process flow and amplification control were simultaneously assessed along with each sample through a triplex assay design provided by the SARS-CoV-2 RT-qPCR detection kit (Promega, WI). Process flow control was assessed through targeting the PMMoV RNA using the Cy5 channel of the RT-qPCR instrument. While some studies advocate using PMMoV as a normalizing gene, our study quantified PMMoV to establish a Cq value range to serve as a benchmark for subsequent reactions. Our preliminary assessment of PMMoV in our wastewater samples from each sampled WWTP established a baseline Cq range of 16-19. Cq shifts of more than 2 or negative PMMoV results signify signs of potential reverse transcription inhibition,

qPCR inhibition, or lab processing error according to the manufacturer's instructions. Amplification control was assessed through the HEX channel by quantifying a 435bp linear DNA template that is pre-mixed in the 20X Primer/Probe/Internal Amplification Control tube. Amplification inhibition is defined by a Cq shift of greater than 3 compared to the no template control according to the manufacturer's instructions. Sample dates flagged for potential inhibition were processed a second time using the replicate samples stored in the -80°C. Replicate RNA extracts were prepared in three concentrations, undiluted, diluted 1:2, and diluted 1:5 before performing the RT-qPCR assay as previously described. Dilutions were carried out using nuclease free water.

Variant Analysis with RT-ddPCR

SARS-CoV-2 variant analysis was carried out on a QX200 AutoDG Droplet Digital PCR (ddPCR) instrument (Bio-Rad, CA). Primers and probes used to detect and discriminate SARS-CoV-2 Alpha variant from the parental Wuhan strain were obtained from the GT dPCR™ Mutation Detection Assays, Validated Kit (GT Molecular, CO). Positive controls for Alpha and Wuhan strains were provided by GT dPCR™ Mutation Detection Assays, Validated kit. Design specifics for the primer and probes from the GT dPCR™ Mutation Detection Assays, Validated Kits are not available and therefore not included in this study. Reaction mixtures consisted of 5 uL RNA extract, 5.5 uL of 2x Super Mix, 1 uL of GT-Primer-Probe Solution 4-Plex, 2.2 uL Reverse Transcriptase, 1.1 uL of DTT, and 7.2 uL of nuclease free water, in a final volume of 22 µL. Each sample was analyzed in duplicates. Non template controls were included in each RT-ddPCR run, where nuclease free water was used in place of the RNA extract. Thermocylcing conditions for all RT-ddPCR reactions were 1 cycle at 50°C for 60, 95°C for 10 min, followed by 45 cycles at 94°C for 30 sec and 60°C for 60 seconds, then 1 cycle at 98°C for 10 min, and 4°C for 30 min. RT-ddPCR results were analyzed using QuantaSoft Analysis Pro software v.1.0 (Bio-Rad, CA).

Contributing Cases by Sewershed

GIS shapefiles of the WWTP sewersheds were obtained from the Los Angeles County Sanitation District (LACSD) and Los Angeles Sanitation and Environment (LASAN). The GIS shapefiles were overlaid onto the shapefile for Countywide Statistical Areas (CSAs), acquired from the Los Angeles County GIS Hub. Using QGIS, the distribution of these CSAs within their corresponding WWTP sewershed was determined. Using this distribution, the proportion of a CSA lying within a given WWTP sewershed was used as a proxy for the portion of cases that CSA contributed to the viral loading of the WWTP. Using data made available by the Los Angeles County Department of Public Health, the new cases per day per CSA were distributed to each of the five WWTPs sampled. New cases per day represents the number of positive tests for the samples collected on each specific date. Only cases within these five sewersheds were counted.

System-Specific Factor Analysis

Influent wastewater quality was obtained from LACSD and Hyperion Water Reclamation Plant. Sampled WWTPs were ranked in respect to each SSF between 1-5, where 1 = highest value and 5 = lowest value. The SSF assessed in this study were total suspended solids (TSS), biochemical oxygen demand$_5$ (BOD_5), population serviced, influent flow rate, new cases, and new cases per influent flow rate for the duration of the study. Our set of SSFs were chosen based on the completeness of their dataset and availability across all sampled WWTPs. Spearman ranked correlation was used to assess the relationship between each SSF-ranked list to a separate ranked list in decreasing Pearson coefficient strength between wastewater SARS-CoV-2 levels and sewershed specific clinical data.

Monte Carlo Simulation

The number of SARS-CoV-2 infected individuals was estimated via Monte Carlo simulations using Oracle Crystal Ball (Version Number 11.1.2.4.850, Redwood City CA). The equation used for our model is presented below(9,21):

$$NIF = Rq*Q/(F*Rf*P)$$

NIF = Estimated number of infected people, Rq = Viral load in wastewater (virus copies/L), Q = Wastewater flow rate (L/day), Rf = Viral load in stool (virus copies/g stool), F = Daily production of stool per capita (g stool/capita-day), and P = % of SARS-CoV-2 infected individual who shed the virus in their stool. While previous studies suggest wastewater SARS-CoV-2 RNA follows a first order decay rate in the sewer lines, a variable parameter for SARS-CoV-2 RNA loss was not included in the model due to the limited number of studies on the decay constant for the sampled sewersheds. Further, the rate loss parameter of wastewater SARS-CoV-2 is further confounded by the report of relatively high wastewater SARS-CoV-2 RNA signal persistence in untreated wastewater(13). In one study, wastewater SARS-CoV-2 RNA signal achieved a persistence of T_{90} = 3.3 to 33 days in untreated wastewater, depending on the wastewater SARS-CoV-2 concentration(13), where T_{90} is the time it takes to lose 90% of the maximum signal. Our omission of the parameter for viral RNA loss simplifies real world conditions and shifts our estimation toward the conversative side. Our estimation can be refined as more representative data emerges.

Data for the 24-hour averaged wastewater flow rate (Q) was provided to us by LACSD and the Hyperion Water Reclamation Plant. Stool viral load (R_f) (virus copies/g) had a log-normal distribution with a mean of 7.18 and standard deviation of 0.67 in $\log_{10}$(22). Daily stool production per capita (F) (g/capita-day) had a log-normal distribution with a mean of 149 and standard deviation of 95 according to reports for high income earning countries(23). The percentage of SARS-CoV-2 infected individuals who shed the virus in their stool (P) was simulated as a uniform distribution from 0.29 to 0.55(24–26). Estimates for each sample point are based on 50,000 simulations.

The median value was used to represent each estimate due to the right skewed probability distribution of the two input variables, R_f and F. The median value is more robust toward

extreme values drawn from the input variables compared to the mean value. Further, the 95% confidence interval (CI) for our estimates were determined through bootstrapping the model using the parameter of 200 experiments and 1,000 simulations each.

Results and Discussion

SARS-CoV-2 Detected in sampled WWTPs

A total of 250 composite influent samples were collected during the period of this study (Table 1). Overall, samples from San Jose Creek Water Reclamation Plant (SJ), Hyperion Water Reclamation Plant (HYP), Joint Water Pollution Control Plant (JW), Whittier Narrows Water Reclamation Plant (WN), and Long Beach Water Reclamation Plant (LB) contained a positivity rate of over 80% for SARS-CoV-2 (202 positive detections/250 samples). As most of the non-detects occurred during the early stage of the pandemic, non-detects were simply omitted from downstream analysis to prevent the possibility of overcorrection. Samples from WN and LB contained more frequent non-detects for SARS-CoV-2 in the early phase of the study compared to the remaining WWTPs. A potential explanation for our observation could be smaller WWTPs require a greater degree of SARS-CoV-2 penetrance within their serviced population for the excreted viral load to rise above the limit of detection of our RT-qPCR assay (1,200 copies/L). In agreement, samples from SJ, HYP, and JW consistently contained higher levels of SARS-CoV-2 than WN and LB due to the larger population serviced by the former three WWTPs. Consistent with previous reports, Pearson correlation analysis of the quantified N1 and N2 genes within each WWTP was strongly correlated to each other $r = 0.90\text{-}0.99$, $p < 0.05$(27) (SI Figure 1)**.**

Wastewater SARS-CoV-2 levels show strong sensitivity and correlation to reported new cases of Covid-19 in Los Angeles County

Wastewater SARS-CoV-2 levels (virus copies/L) for Los Angeles County were obtained by using the mean value from all sampled WWTPs for each date. In addition, all datasets were smoothed using a non-parametric regression to reduce background noise. Smoothing was done in XLSTAT (Addinsoft) using the built-in Brown's linear exponential smoothing function, with 500 iterations and self-optimized alpha value. Since measurable wastewater SARS-CoV-2 levels are known to vary due to several external factors such as variable viral load, wastewater flows, wastewater quality, collection protocol, and lab processing method, statistical smoothing was used to denoise the imperfect and variable datasets and highlight general patterns. Smoothing of the datasets improved the correlation coefficient between wastewater SARS-CoV-2 levels and new cases from r_{raw}=0.87 N1 and 0.88 N2, $p << 0.01$ to r_{smooth} =0.94 N1 and 0.94 N2, $p << 0.01$. Consistent with previous studies, our measured wastewater SARS-CoV-2 levels reflect reported new cases of Covid-19 to its corresponding regions(8,28). The two major surges of new Covid-19 cases in Los Angeles County at the beginning of June and November 2020 coincide with elevated levels of wastewater SARS-CoV-2 during the same period (Figure 2). Interestingly, during both summer (June 2020) and winter (November 2020) Covid-19 outbreaks, wastewater SARS-CoV-2 levels showed high sensitivity toward the accumulation

and decline of reported average daily new cases. From June 2nd to July 28th, 2020, wastewater SARS-CoV-2 levels increased by roughly 64,000 virus copies/L (530%) from a corresponding increase of 1,722 average daily new cases (120%). Similarly, from November 3rd to January 18, 2021, wastewater SARS-CoV-2 levels increased by more than 2 million virus copies/L (>1,500%) from an increase of 9,943 averaged daily new cases (500%). As the infection rate fell following the summer peak, July 28th to August 11th, 2020, wastewater SARS-CoV-2 levels decreased by 210,000 virus copies/L (54.6%) and then 85,000 virus copies/L (48.7%) in the first and second week, respectively, which correspond to a decline in the average daily new cases by 434 (13.8%) and then 363 average daily new cases (13.3%) over the same period. The steep increase in wastewater SARS-CoV-2 levels in response to rising daily new cases is likely due to the fecal SARS-CoV-2 pattern, where fecal viral titers peak in the first 1-2 weeks after the onset of symptoms followed by a steady decline in the following weeks(29). Therefore, wastewater SARS-CoV-2 levels are sensitive to rising and falling community infections rates, which makes WBE suitable for community-level surveillance.

Interestingly, a recent WBE study in Southern California overlapped with our sampling period by approximately 30 weeks and allows a unique opportunity to compare WBE data from two independent labs sampling from the same WWTPs (JW and SJ)(28). Despite significantly different sample processing methods between the two labs (direct extraction, Qiamp Viral RNA kit, and recovery adjusted data versus HA filtration, Maxwell 16 LEV simply RNA blood purification kit, and unadjusted data), reported wastewater SARS-CoV-2 levels from both labs captured the summer and winter surge of Covid-19 cases in Los Angeles County. Moreover, the overall similar wastewater SARS-CoV-2 trend in both studies suggest temporal measured wastewater SARS-CoV-2 data can be presented in its unadjusted form if proper process and inhibition controls are done.

Wastewater SARS-CoV-2 levels strongly correlates to the average new cases by contributing sewershed

Data from the Covid-19 Dashboard for Los Angeles County was separated by CSA to obtain a representative dataset for the sewershed corresponding to each sampled WWTP. Again, all datasets were smoothed using a non-parametric regression analysis to reduce background noise. Pearson correlation analysis for both raw and smoothed datasets were strongly correlated to the averaged new cases of each respective sewershed. In every case, smoothing increased the correlation coefficient (Pearson r_{raw} = 0.45-0.85, $p << 0.01$ and Pearson r_{smooth} = 0.76-0.95, $p << 0.01$, Figure 2). Interestingly, the average daily new cases across all sampled sewersheds rose and fell around similar dates during the summer and winter peaks. The near-synchronous wave of averaged daily new cases in the sampled communities could likely be explained by the highly infectious nature of SARS-CoV-2(30), the extensive traveling between neighboring communities within Los Angeles County, and large centralized WWTPs that service multiple zip codes. While previous WBE studies conducted in areas with smaller decentralized WWTPs could provide greater geographic resolution due to their smaller sewershed size, here we demonstrate large centralized WWTPs can provide insights for communal SARS-CoV-2 load

in sewersheds serving up to 4 million people without compromising the sensitivity to reflect corresponding clinical case counts.

We acknowledge a level of uncertainty in splitting LA County Covid-19 Dashboard data by CSA for comparison between sewershed-specific case counts and its respective wastewater SARS-CoV-2 level. Our approximation of the sewershed boundaries is confounded by the interconnected sewer lines and broadly defined sewershed borders within LACSD. For instance, LACSD WWTPs that are upstream of JW (Whittier Narrows, San Jose Creek, and Long Beach Water Reclamation Plant) are designed to divert excess wastewater to JW as part of their overflow management practice and could dilute or enrich the wastewater SARS-CoV-2 level in JW. However, from a size perspective, JW treats an averaged influent flow rate of 305 MLD, which is one or two orders of magnitude greater than the average influent flow rate of SJ (36.8 MLD), LB (16.5 MLD), and WN (9.87 MLD), which could make measured wastewater SARS-CoV-2 levels in JW robust toward dilution or enrichment effects from upstream LACSD WWTPs, under non-extreme conditions. Further, wastewater in LACSD is designed to flow southwest which adds confidence that wastewater SARS-CoV-2 levels for WN, SJ, and LB, which are upstream of JW, should be largely unaffected by non-regional wastewater.

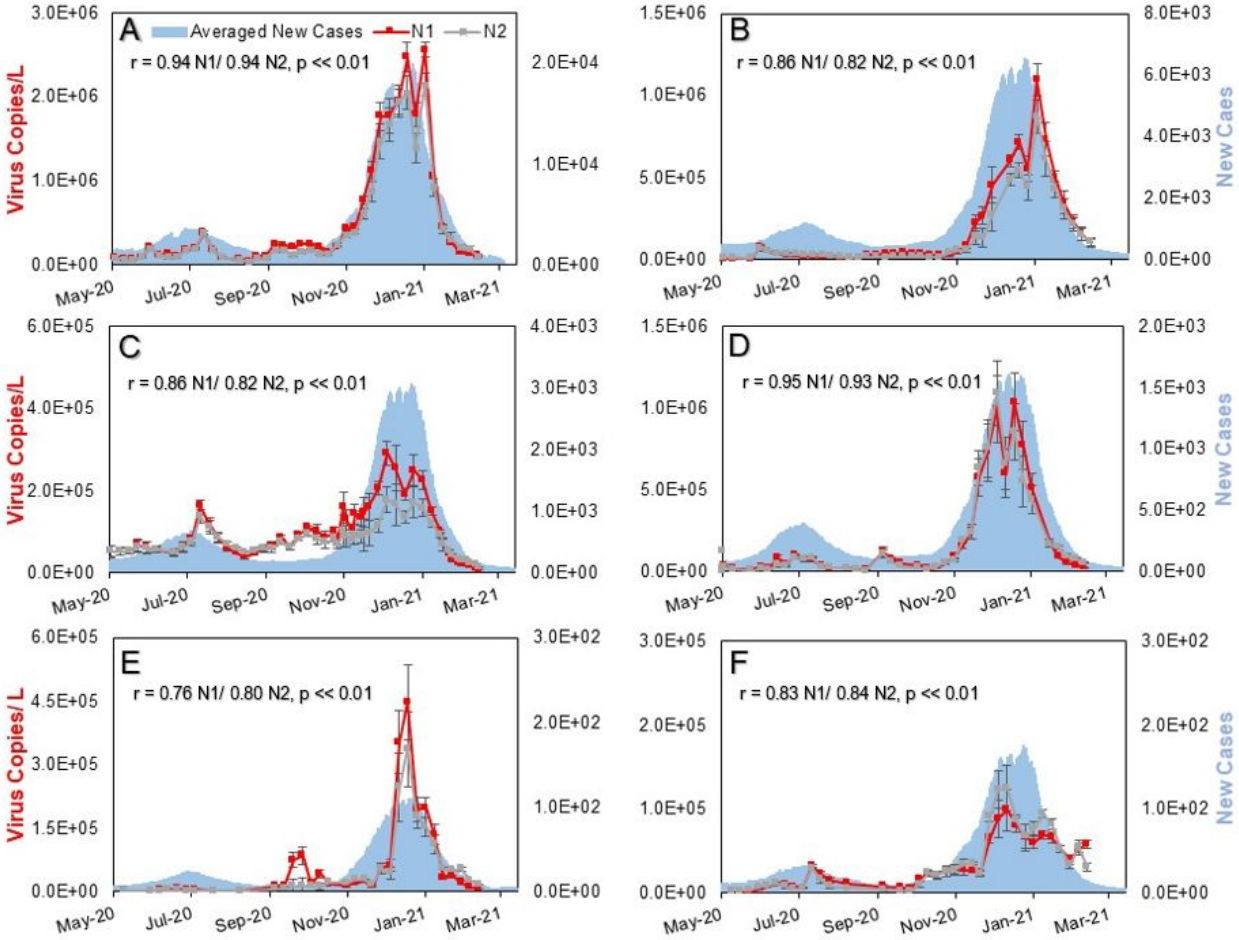

Figure 2A-F: 2A) Time series analysis of the averaged viral copies/L for all sampled WWTPs and averaged new cases rate for Los Angeles County over the duration of this study. 2B-F) Time series analysis of SARS-CoV-2 viral copies/L for each sampled

WWTP and the averaged new positive tests for the respective sewershed. Dark red line represents quantified N1 data, pink line represents quantified N2 data and blue bar chart represents the moving seven-day average of daily new cases A= Total, B=HYP, C=JW, D=SJ, E=LB, and F= WN. Error bars represent the standard deviation of the measured N1 or N2 value. Pearson coefficient r represents the correlation between the N1 or N2 gene copies/L and regional clinical data.

Comparison of daily viral load to 20-day case count could help identify under testing communities

We compared the daily viral load to a moving 20-day case count in each sewershed to assess the variability between measured wastewater SARS-CoV-2 levels and clinical data over the course of this study. Our motivation for this comparison stems from the length of our WBE work, which allowed us to compare the relationship between our WBE data to different stages of the pandemic as public perception and participation toward in-person testing evolved over the course of this 44-week study. Compared to WBE, in-person testing is likely more susceptible to public perception and preparedness such as education, testing availability, and fatigue. Although the reported SARS-CoV-2 shedding period in stool ranges from 1-47 days, the general consensus places the mean shedding period to be around 12-20 days(31,32). Therefore, we used the number of reported cases within a 20-day window to represent the viral shedding population. Viral load for each WWTP was calculated by multiplying measured virus copies/L by averaged influent flowrate (MLD) on each date. In general, larger sewersheds (HYP, JW, and SJ) exhibited a lower ratio and variability compared to smaller sewersheds (LB and WN, Figure 3A). The observed pattern could be the result of large sewersheds having a higher testing capacity and participation than smaller sewersheds. Limited testing capacity or participation poses a risk of under reporting or overlooking disease outbreaks.

For greater temporal resolution, we divided our analysis into three segments, June-August 2020, September-October 2020, and November 2020-March 2021 (Figure 3B-D). Segments were divided based on timeframes that allow comparisons of individual outbreaks. During June-August 2020, the ratio and variability of viral load to the moving 20-day case count for each sampled sewershed was inversely related to the size of the serviced population (Figure 3B), which is consistent with our previous explanation. For HYP, JW, SJ, LB, and WN, the median ratios were 0.8, 8.3, 9.3, 10.3 and 21.8, respectively. During September-October, the median ratio of daily viral load to the moving 20-day case count increased by 80-320% for HYP, JW, SJ, and WN and 2,700% for LB compared to the ratios during June-August 2020. While the increased ratios for HYP, JW, SJ, and WN during September-October is likely attributed to the decline in administered Covid-19 tests in September compared to August (SI Figure 2), the stark increase of 2,700% in LB suggests potential under reporting of a resurgence in LB following the summer peak. On closer examination, the moving 20-day case count in LB steadily declined in the first half of September and reached a low of 141 cases on September 17th. Afterwards, the moving 20-day case count reached a peak of 156 cases on October 1st, which represents an increase of 15 new cases from September 17th and could likely be considered insignificant. However, over a similar period the viral load for LB increased from < 9,000 virus copies/day to 1.2 million virus copies/day (September 15th-October 6th, 2020). Based on the discrepancy between the 20-day case count and the daily viral load seen in LB, future WBE implementations could be used to validate clinical data for sewersheds where testing capacity

and participation are likely strained. From November-March 2021, the median ratio of daily viral load to the 20-day case count decreased by 83.3%, 81.2% and 37.4% for JW, LB, and WN, respectively, compared to ratios from September-October. The decreased median ratios for JW, LB, and WN is likely due to the record number of Covid-19 tests administered during November-March 2021. Surprisingly, the median ratio of daily viral load to the moving 20-day case count increased by 39.3% and 18.2% for SJ and HYP, respectively, which could be due to the rate of new infections exceeding the increased Covid-19 tests performed in SJ and HYP. While the relationship between viral load and infected individuals is highly variable, monitoring the daily viral load to the moving 20-day case count in each sewershed over time could help identify under testing communities. We acknowledge that our analysis would require additional studies for validation. For instance, sudden shifts to high fecal-viral load SARS-CoV-2 variants in the infected population my cause an inflation to the ratio of wastewater SARS-CoV-2 to 20-day case count. Ongoing data for community-specific SARS-CoV-2 variant profile would help refine our analytical approach. Further, our assumption for a fixed 20-day period to estimate the number of active cases is subject to change as additional high-quality data for the recovery window recovery continues to surface.

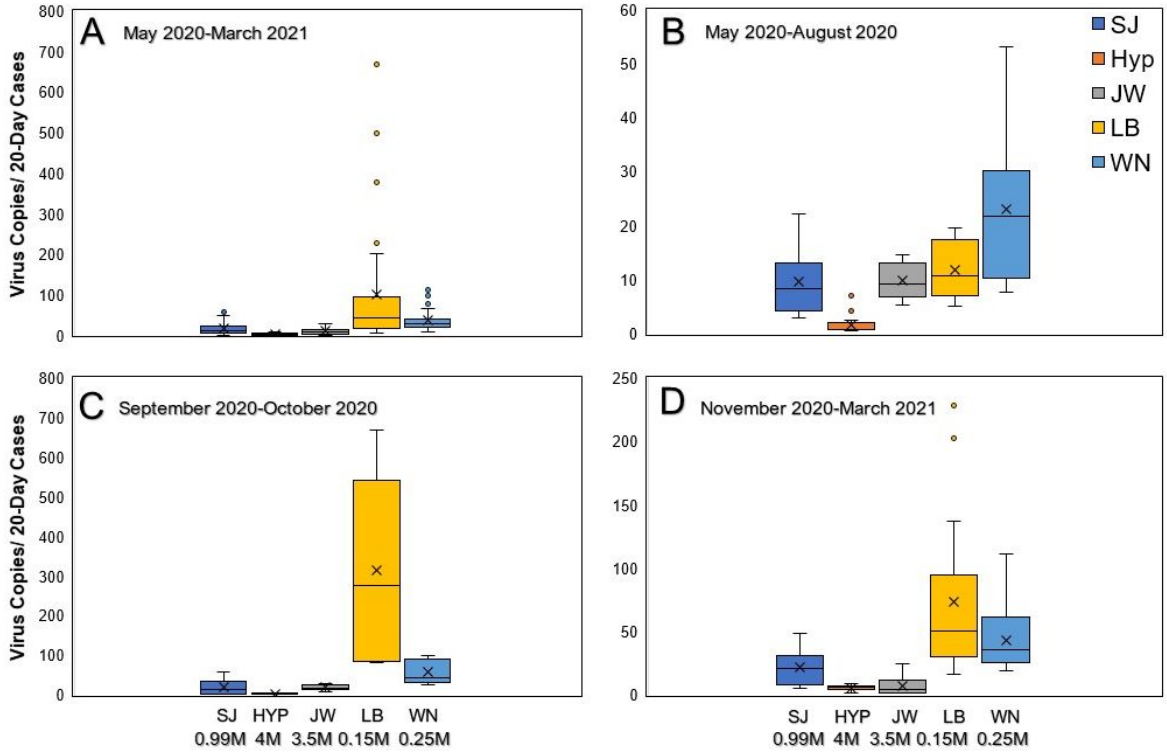

Figure 3A-D: Box plot analysis of daily viral load to the moving 20-day case count for each sampled sewershed. 3A) The duration of the study May 2020-March 2021 3B) May- August 2020 3C) September-October 2020 3D) November-March 2021. Box represents the median, 25th, and 75th percentile. The whiskers represent the largest and smallest values and outliers are shown as circles. Error bars represent standard deviation.

Clinical cases normalized by influent flow rate, TSS, and BOD5 are potential factors that may influence Wastewater SARS-CoV-2 Correlation to clinical data

Interestingly, the Pearson correlation strengths between the wastewater SARS-CoV-2 level of each sampled WWTP and its respective regional new cases did not follow any obvious trend. While HYP and JW are the two largest WWTPs sampled (941 and 305 MLD, respectively), the corresponding Pearson coefficient (r_{smooth} = 0.90 N1 /0.87 N2 and 0.82 N1/ 0.80 N2, $p << 0.01$) ranks 2nd and 4th in our dataset. Whereas SJ being the third largest WWTP sampled (36.8 MLD) displayed the strongest Pearson coefficient (r_{smooth}= 0.94 N1/ 0.91 N2, $p << 0.01$). Further, WN (9.83 MLD) treats significantly less wastewater than HYP and JW, but its Pearson coefficient (r_{smooth}= 0.85 N1/ 0.88 N2 $p << 0.01$) is comparable to HYP and stronger than JW. To assess SSFs that may influence the correlative strength of wastewater SARS-CoV-2 levels to clinical data, we ranked our sampled WWTPs, in decreasing Pearson coefficient, and compared it to individual lists of sampled WWTPs, each ranked in respect to one SSF. The SSF examined in this study were TSS, BOD_5, serviced population size, averaged influent flowrate, new cases, and new cases per averaged influent flowrate. In total, seven ranked lists were created, one list ranked by decreasing Pearson coefficient and six lists each ranked by one SSF in decreasing value. Spearman ranked correlations were used to assess the relationship between the Pearson coefficient ranked list to the SSF ranked lists. Based on our assessment, new cases normalized by average influent flow rate showed a very strong relationship to the Pearson coefficient ranking between wastewater SARS-CoV-2 levels and regional new cases ($r = 0.9$ and $p < 0.05$, Table 2B). While TSS and BOD_5 showed strong relationship ($r = 0.06$, $p > 0.05$, Table 2B) to the Pearson coefficient ranking between wastewater SARS-CoV-2 levels and regional new cases, our dataset of fived sampled WWTPs did not reach statistical significance of p-value < 0.05. However, given previous reports of higher wastewater SARS-CoV-2 detection in biosolids compared to primary influent(33) and a positive association of coronavirus survival rate with biosolids and organic matter concentrations(34), we encourage future studies to conduct a similar analysis with a greater number of WWTPs. Overall, correlative strength between wastewater SARS-CoV-2 and clinical data is most strongly influenced by the ratio of new cases per averaged influent flowrate, whereas TSS and BOD_5 levels showed potential strong relationship. While we acknowledge that the p values for the TSS and BOD_5 analysis presented here are greater than the commonly accepted $p = 0.05$, we believe increasing levels of TSS and BOD_5 would facilitate the adsorption of wastewater SARS-CoV-2 to particulates. An increased fraction of adsorbed SARS-CoV-2 could increase the measurable wastewater SARS-CoV-2 fraction and improve the correlative strength between wastewater SARS-CoV-2 levels to regional new cases. Further, concentrating solids in primary influent may be a viable alternative for WWTPs that serve areas with a low number of Covid-19 cases or a low ratio of Covid-19 cases per averaged influent flow rate.

Table 2A-B: 2A) Summary table representing the ranking of the Pearson Correlation coefficient of all sampled WWTPs to regional clinical cases. 1 = highest Spearman correlation coefficient and 5 = lowest Spearman correlation coefficient 2B) Summary table of the Spearman rank correlation coefficient of each SSF to the Pearson Correlation ranking of each sampled WWTPs.

A Utility	Clinical and Wastewater Correlation Ranking	B Correlation of SSF to Clinical and Wastewater Correlation Ranking
		New Cases/MLD

SJ	1	r = 0.9, p < 0.05
JW	2	BOD_5 r = 0.6, p > 0.05
WN	3	TSS r = 0.6, p > 0.05
HYP	4	New Cases r = 0.3, p > 0.05
LB	5	Population r = 0.1, p > 0.05
		Average MLD r = 0.1, p > 0.05

Daily Wastewater sample could lead clinical data by up to five days

Although previous studies report wastewater and primary sludge SARS-CoV-2 levels lead clinical and hospitalization cases by 0-6 day(27,35), our dataset showed no significant signs of lead time when offsetting measured wastewater SARS-CoV-2 levels to the daily new cases for JW. The initial assessment was done using the wastewater SARS-CoV-2 data for JW for each month and by complete dataset. We hypothesized that the short 0-2 day lead time in wastewater SARS-CoV-2 may have been lost when sampling once or twice a week. To examine the potential lead time of wastewater SARS-CoV-2 to reported daily cases, we collected daily composite influent samples from JW from August 16th, 2020 to August 22nd, 2020 and compared our results to the daily new COVID-19 cases corresponding to the JW sewershed. The comparison was done by aligning measured SARS-CoV-2 levels to the reported daily new cases on the same day of sample collection or by offsetting the two datasets from 1-5 days. Pearson correlation analysis of daily wastewater SARS-CoV-2 levels to same day daily new cases showed a correlation coefficient of r_{smooth}=0.81 N1/0.69 N2, $p < 0.05$ N1 and $p > 0.05$ N2. However, offsetting the reported daily new cases by 5 days improved the correlation coefficient to r_{smooth} = 0.96 N1/0.96 N2, $p < 0.005$ (Figure 4A and 4B). Interestingly, offsetting the reported daily new cases by 2 days also improved the correlation coefficient to r_{smooth} = 0.91 N1/ 0.92 N2, $p < 0.05$, whereas offsetting the reported daily new cases by 1, 2, and 3 days showed decreased or mixed improvement to the correlation coefficient (r_{smooth} = 0.78 N1/ 0.77 N2 $p <$ 0.05, r_{smooth} = 0.78 N1/ 0.82 N2 $p < 0.05$, r_{smooth} = 0.72 N1/ 0.71 N2 $p > 0.05$, respectively. In agreement with our hypothesis, future WBE implementation using daily sampling could offer improved sensitivity in detecting early rises in community infections compared to weekly samples. While the increased correlation coefficient through temporal offsetting the daily reported new cases by 2 and 5 days highlights the susceptibility of our comparison to spurious correlations, future studies can limit this shortcoming by increasing the number of samples collected over a greater number of WTTPs.

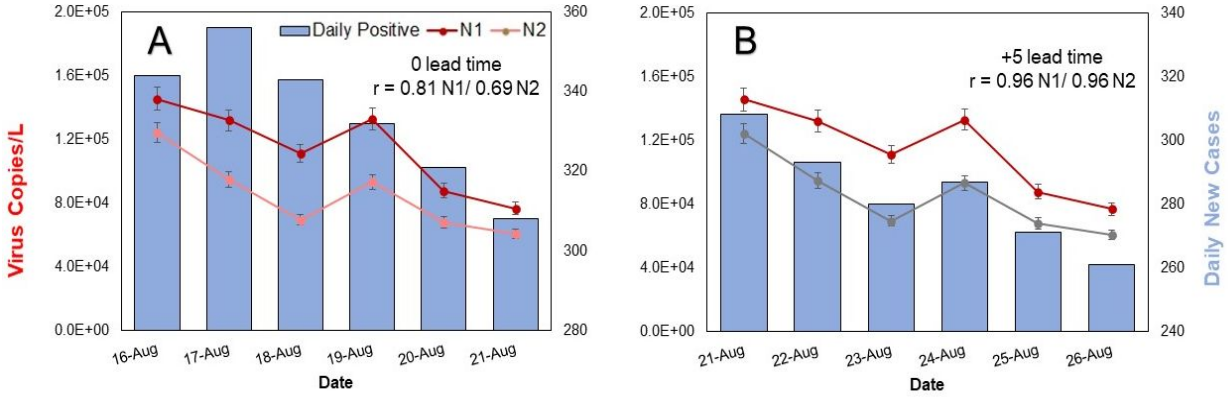

Figure 4A-B: Comparison of daily wastewater SARS-CoV-2 virus copies/L (N1=red and N2= grey) from JW to its respective daily new cases (blue). 4A) Represents same day comparison. 4B) Represents measured SARS-CoV-2 virus copies/L compared to the daily new cases five days later. Error bars represent standard deviation.

Variant Analysis

At the time of our study, reports of SARS-CoV-2 variants began to emerge around the United States(36). Specifically, the novel B.1.1.7 variant or UK variant was reported to be more infectious than the original Wuhan strain(36–38). The highly infectious nature of the UK variant caused some experts to estimate its dominant circulation in the United States by March 2020(36). To showcase the utility of WBE to assess communal variant composition, select replicate extracts from HYP and JW were analyzed for the UK variant by quantifying the presence of the point mutation 501Y and del 69-70(37). Each sample was benchmarked to the presence of the Wuhan strain by measuring the targets N501 and HV69-70. Variant analysis was performed using reverse transcription droplet digital PCR (RT-ddPCR) due to its reported lower limit of detection than RT-qPCR. Despite reports of increasing prevalence of the UK variant in sequenced clinical samples in the United States (https://www.gisaid.org/hcov19-variants/), we did not detect the UK variant in any of our samples. Although we did not detect the UK variant in our select samples, we cannot conclude the absence of any UK variant infections in Los Angeles County during the time of our study. While the relative abundance of the UK variant among sequenced SARS-CoV-2 strains reached a high of 14% around March 1, 2021, the averaged new cases of Covid-19 in Los Angeles County on March 1, 2020 fell to 1.16E+03 cases, which marks a 90% reduction from its all-time high. The viral load from the UK infections within the declining case count in March 2021 were likely further diluted in communal waste streams to below the limit of detection of our RT-ddPCR assay (10 copies/reaction). Quantified Wuhan variant concentrations were comparable to our qPCR results (data not shown), which suggests both RT-qPCR and RT-ddPCR are suitable assays to measure wastewater SARS-CoV-2. For future studies, we recommend metagenomic sequencing of wastewater samples as a preliminary step to assess all possible variant strains and their relative abundance to better customize the selection of variant targets for each geographical region.

Estimated Infected Population from Monte Carlo Simulations Exceed the Reported Clinical Cases by more than 200 Percent

Monte Carlo simulations were used to estimate the median number of infected individuals (NIF) for Los Angeles County and for the sewershed of each sampled WWTP. A total of 50,000 simulations were performed for each data point. Here we report a summary of the median NIF obtained from the simulations. Summary results from the simulation are presented in Table 3. Full results from the simulation can be found in SI Table 2. We used a conservative 20-day window to estimate the cumulative NIF for Los Angeles County. Our simulation estimates the peak NIF for Los Angeles County to be 1.25 million (95% CI: 4.91E+05 - 3.55E+06), which occurred on January 19th, 2021 (Table 3). In contrast, the cumulative reported case count for the 20-days leading up to January 19th was 2.08E+05 people, which falls short of the simulated NIF by a factor of 6. As expected, the simulated NIF are well above the reported case counts and demonstrates the potential utility of WBE to consistently sample a far greater population than in-person testing.

Our estimate raises the prevalence of Covid-19 from 14.5% to 34.2% for Los Angeles County. Using a 20-day window, we estimate the cumulative NIF in Los Angeles County to be around 3.42 million people (95% CI: 7.91E+05 - 9.12E+06) from the period between May 2020 to March 2021. Our estimate exceeds the 1.45 million reported cases over the same duration by more than a factor of 2. While we acknowledge there are multiple uncertainties in our prediction, we believe our estimate to be on the conservative side due to the inevitable viral loss through the sewer networks and sample processing that were not factored into the simulation. For instance, the HA filtration method used to concentrate wastewater samples in this study has a reported extraction efficiency between 27.3-60.5% ± 22.2%(18,19). Adjusting our estimate by a fixed extraction efficiency of 60.5% would increase the cumulative NIF estimate to 5.7 million people. However, since we did not track extraction efficiency during this study our estimate remains 3.42 million people (95% CI: 7.91E+05 - 9.12E+06). Interestingly, our Covid-19 prevalence estimate of 34.2% closely resembles the 37.5% prevalence estimate reported by Los Angeles Health Services and the 30-50% prevalence estimate by previous reports(39,40).

Table 3: Summary values of the peak median NIF, 95% CI, and peak date from the Monte Carlo simulations using 50,000 simulations per datapoint.

Sewershed	Peak Median NIF	95% Confidence Interval	Peak Date
SJ	5.17E+04	(1.89E+04 -1.41E+05)	December 22nd, 2020
HYP	1.17E+06	(4.33E+05 - 3.23E+06	January 19th, 2021
JW	9.04 E+04	(3.54E+04 - 2.39E+05)	December 22nd, 2020
LB	8.45E+03	(3.20E+03 - 2.46E+04)	January 5th, 2021
WN	1.43E+03	(5.27E+02 - 3.69E+03)	December_29th, 2020
Aggregate	1.25E+06	(4.91E+05 - 3.55E+06)	January 19th, 2021

Using the same 20-day window, we estimate the total number of infected individuals for SJ, HYP, JW, LB, and WN to be 1.21E+04, 4.4E+05, 1.53E+04, 5.94E+03, and 3.57E+03 per 100,000 people, respectively. Based on our simulation, the highest NIF per 100,000 people occurred in the catchment area belonging to HYP, followed by JW, SJ, LB, and WN (Figure 5). In contrast to our simulation, the reported public health data (separated by sewershed) ranked SJ to have the highest rate of infection, followed by HYP, WN, JW, and LB. We believe the disagreement in our simulated ranking versus the public health data stems from the uncertainty surrounding the true infected population. If the true infected population lies closer to 1.45 million people or 14.4% of the population in Los Angeles County, then the adjusted case rate should have hot spots and follow the public health data. However, if the true infected population is far more prevalent and closer to 3.42–5.7 million people or 34.2- 57% of the population in Los Angeles County, then the infections are likely less concentrated in one community and the adjusted rate would likely mirror the ranking for serviced population size.

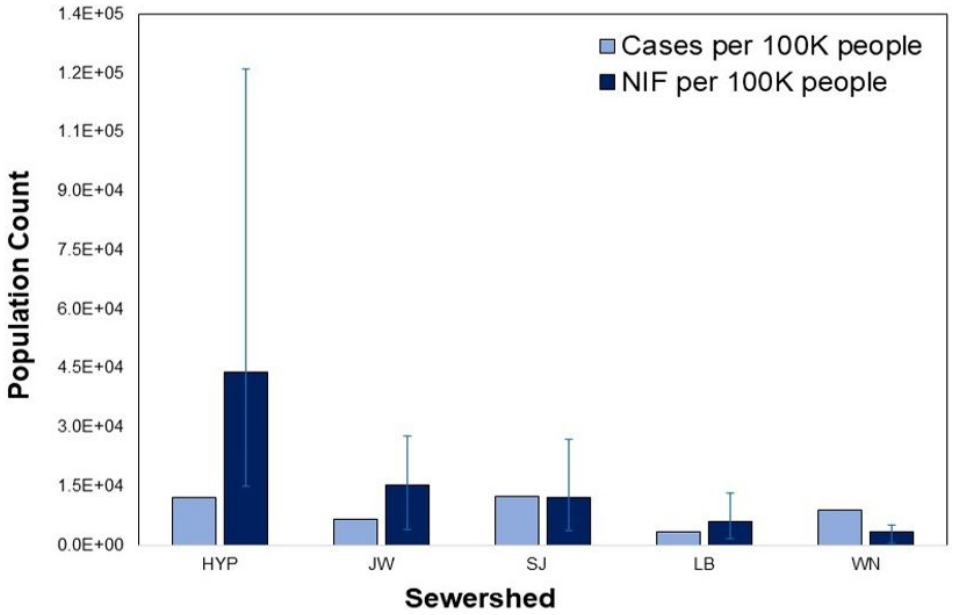

Figure 5: Comparison of the reported adjusted cases per 100,000 people (light blue) vs. simulated NIF per 100,000 people (dark blue). Error bars represent the 95% CI.

We acknowledge that the model used for our estimate requires further calibration and should not be taken as an absolute calculation for the infected population. Further, variations in lab processes, sample handling experience, and SARS-CoV-2 variant profile could significantly alter the input parameters and the estimated output. However, despite the uncertainties listed, we believe Monte Carlo simulations using measured wastewater SARS-CoV-2 can be beneficial to the improvement of future models as more specific and representative data emerges. Monte Carlo simulations can be another option in the suite WBE tools that can be used to complement clinical data.

Conclusion

In this comprehensive study, we demonstrate the utility of WBE for SARS-CoV-2 using various approaches ranging from RT-qPCR to statistical estimation. We first quantified wastewater SARS-CoV-2 levels in Los Angeles County and showcased the effectiveness of WBE to track regional SARS-CoV-2 load for communities ranging from 150,000 to 4,000,000 people. While measured wastewater SARS-CoV-2 concentrations varied from sample-to-sample, smoothing the dataset was effective in denoising background variability to reveal the general trend of wastewater SARS-CoV-2 levels over time. Further, wastewater SARS-CoV-2 trends measured from daily samples may lead reported daily new cases by 2 or 5 days. SSF such as dilution factors should be considered for future WBE implementation as the ratio of new cases to averaged influent flowrate is a better indicator of correlation strength than serviced population size, averaged influent flowrate, TSS, and BOD_5. Measured wastewater SARS-CoV-2 data were used to estimate the median NIF via Monte Carlo simulations. Our simulation estimates the largest active infection population peaked on January 19th, 2021 with 1.25 million NIF (95% CI: 4.91E+05 - 3.55E+06) and a total of 3.42 million NIF (95% CI: 7.91E+05 - 9.12E+06) between the period of May 2020-March 2021 (34.2% of Los Angeles County's population). In comparison to the reported case count, our simulated infected population exceeds the reported number of cases by almost 2 million people.

Conflicts of interest

We do not have any conflicts of interest to declare.

Acknowledgements

The figure for the table of contents entry was adapted from "Quantifying SARS-CoV-2 Virions in City Wastewater", by BioRender.com (2021). Retrieved from https://app.biorender.com/biorender-templates. Figure 2B was created with Biorender.com.

References

1. Arora S, Nag A, Sethi J, Rajvanshi J, Saxena S, Shrivastava SK, et al. Sewage surveillance for the presence of SARS-CoV-2 genome as a useful wastewater based epidemiology (WBE) tracking tool in India. Water Sci Technol. 2020;82(12).
2. Polo D, Quintela-Baluja M, Corbishley A, Jones DL, Singer AC, Graham DW, et al. Making waves: Wastewater-based epidemiology for COVID-19 – approaches and challenges for surveillance and prediction. Water Res. 2020;186.
3. Overview of Testing for SARS-CoV-2 (COVID-19) | CDC [Internet]. [cited 2021 Jun 23]. Available from: https://www.cdc.gov/coronavirus/2019-ncov/hcp/testing-overview.html
4. Crits-Christoph A, Kantor RS, Olm MR, Whitney ON, Al-Shayeb B, Lou YC, et al. Genome sequencing of sewage detects regionally prevalent SARS-CoV-2 variants. MBio.

2021;12(1).
5. Beresford-Jones BS, Shao Y. Through the gut, down the drain. Vol. 19, Nature Reviews Microbiology. 2021.
6. Kocamemi BA, Kurt H, Hacıoglu S, Yaralı C, Saatci AM, Pakdemirli B. First data-set on SARS-CoV-2 detection for istanbul wastewaters in Turkey. medRxiv. 2020.
7. Döhla M, Wilbring G, Schulte B, Kümmerer BM, Diegmann C, Sib E, et al. SARS-CoV-2 in environmental samples of quarantined households. medRxiv. 2020.
8. Medema G, Heijnen L, Elsinga G, Italiaander R, Brouwer A. Presence of SARS-Coronavirus-2 RNA in Sewage and Correlation with Reported COVID-19 Prevalence in the Early Stage of the Epidemic in the Netherlands. Environ Sci Technol Lett. 2020;7(7):511–6.
9. Ahmed W, Angel N, Edson J, Bibby K, Bivins A, O'Brien JW, et al. First confirmed detection of SARS-CoV-2 in untreated wastewater in Australia: A proof of concept for the wastewater surveillance of COVID-19 in the community. Sci Total Environ. 2020 Aug 1;728:138764.
10. Hata A, Honda R, Hara-Yamamura H, Meuchi Y. Detection of SARS-CoV-2 in wastewater in Japan by multiple molecular assays-implication for wastewater-based epidemiology (WBE). medRxiv. 2020.
11. Wu F, Xiao A, Zhang J, Moniz K, Endo N, Armas F, et al. SARS-CoV-2 titers in wastewater foreshadow dynamics and clinical presentation of new COVID-19 cases. medRxiv. 2020.
12. Weidhaas J, Aanderud ZT, Roper DK, VanDerslice J, Gaddis EB, Ostermiller J, et al. Correlation of SARS-CoV-2 RNA in wastewater with COVID-19 disease burden in sewersheds. Sci Total Environ. 2021;775.
13. Gupta S, Parker J, Smits S, Underwood J, Dolwani S. Persistent viral shedding of SARS-CoV-2 in faeces – a rapid review. Vol. 22, Colorectal Disease. 2020.
14. Foladori P, Cutrupi F, Segata N, Manara S, Pinto F, Malpei F, et al. SARS-CoV-2 from faeces to wastewater treatment: What do we know? A review. Sci Total Environ. 2020;743.
15. Li X, Zhang S, Shi J, Luby SP, Jiang G. Uncertainties in estimating SARS-CoV-2 prevalence by wastewater-based epidemiology. Vol. 415, Chemical Engineering Journal. 2021.
16. Haramoto E, Kitajima M, Katayama H, Ito T, Ohgaki S. Development of virus concentration methods for detection of koi herpesvirus in water. J Fish Dis. 2009;
17. Ahmed W, Harwood VJ, Gyawali P, Sidhu JPS, Toze S. Comparison of Concentration Methods for Quantitative Detection of Sewage-Associated Viral Markers in Environmental Waters. Schaffner DW, editor. Appl Environ Microbiol [Internet]. 2015 Mar 15;81(6):2042 LP – 2049. Available from: http://aem.asm.org/content/81/6/2042.abstract
18. LaTurner ZW, Zong DM, Kalvapalle P, Gamas KR, Terwilliger A, Crosby T, et al. Evaluating recovery, cost, and throughput of different concentration methods for SARS-CoV-2 wastewater-based epidemiology. Water Res [Internet]. 2021/03/15. 2021 Jun 1;197:117043. Available from: https://pubmed.ncbi.nlm.nih.gov/33784608
19. Ahmed W, Bertsch PM, Bivins A, Bibby K, Farkas K, Gathercole A, et al. Comparison of virus concentration methods for the RT-qPCR-based recovery of murine hepatitis virus, a surrogate for SARS-CoV-2 from untreated wastewater. Sci Total Environ [Internet]. 2020/06/05. 2020 Oct 15;739:139960. Available from: https://pubmed.ncbi.nlm.nih.gov/32758945
20. Kantor RS, Nelson KL, Greenwald HD, Kennedy LC. Challenges in Measuring the Recovery of SARS-CoV-2 from Wastewater. Vol. 55, Environmental Science and Technology. 2021.
21. Hasan SW, Ibrahim Y, Daou M, Kannout H, Jan N, Lopes A, et al. Detection and

738 quantification of SARS-CoV-2 RNA in wastewater and treated effluents: Surveillance of
739 COVID-19 epidemic in the United Arab Emirates. Sci Total Environ [Internet].
740 2021;764:142929. Available from:
741 https://www.sciencedirect.com/science/article/pii/S0048969720364597
742 22. Lescure FX, Bouadma L, Nguyen D, Parisey M, Wicky PH, Behillil S, et al. Clinical and
743 virological data of the first cases of COVID-19 in Europe: a case series. Lancet Infect Dis.
744 2020;20(6).
745 23. Rose C, Parker A, Jefferson B, Cartmell E. The Characterization of Feces and Urine: A
746 Review of the Literature to Inform Advanced Treatment Technology. Crit Rev Environ Sci
747 Technol [Internet]. 2015 Sep 2;45(17):1827–79. Available from:
748 https://doi.org/10.1080/10643389.2014.1000761
749 24. Cheung KS, Hung IFN, Chan PPY, Lung KC, Tso E, Liu R, et al. Gastrointestinal
750 Manifestations of SARS-CoV-2 Infection and Virus Load in Fecal Samples From a Hong
751 Kong Cohort: Systematic Review and Meta-analysis. Gastroenterology. 2020;159(1).
752 25. Wu Y, Guo C, Tang L, Hong Z, Zhou J, Dong X, et al. Prolonged presence of SARS-CoV-
753 2 viral RNA in faecal samples. Lancet Gastroenterol Hepatol [Internet]. 2020 May 1 [cited
754 2021 Jun 11];5(5):434–5. Available from:
755 https://www.thelancet.com/journals/langas/article/PIIS2468-1253(20)30083-
756 2/fulltext#.YMO6YQRZEF8.mendeley
757 26. Wang W, Xu Y, Gao R, Lu R, Han K, Wu G, et al. Detection of SARS-CoV-2 in Different
758 Types of Clinical Specimens. JAMA [Internet]. 2020 May 12;323(18):1843–4. Available
759 from: https://doi.org/10.1001/jama.2020.3786
760 27. Peccia J, Zulli A, Brackney DE, Grubaugh ND, Kaplan EH, Casanovas-Massana A, et al.
761 Measurement of SARS-CoV-2 RNA in wastewater tracks community infection dynamics.
762 Nat Biotechnol. 2020;38(10).
763 28. Song Z, Reinke R, Hoxsey M, Jackson J, Krikorian E, Melitas N, et al. Detection of
764 SARS-CoV-2 in Wastewater: Community Variability, Temporal Dynamics, and Genotype
765 Diversity. ACS ES&T Water. 2021;1(8).
766 29. Sethuraman N, Jeremiah SS, Ryo A. Interpreting Diagnostic Tests for SARS-CoV-2. Vol.
767 323, JAMA - Journal of the American Medical Association. 2020.
768 30. Elrashdy F, Redwan EM, Uversky VN. Why covid-19 transmission is more efficient and
769 aggressive than viral transmission in previous coronavirus epidemics? Vol. 10,
770 Biomolecules. 2020.
771 31. van Doorn AS, Meijer B, Frampton CMA, Barclay ML, de Boer NKH. Systematic review
772 with meta-analysis: SARS-CoV-2 stool testing and the potential for faecal-oral
773 transmission. Vol. 52, Alimentary Pharmacology and Therapeutics. 2020.
774 32. Cevik M, Tate M, Lloyd O, Maraolo AE, Schafers J, Ho A. SARS-CoV-2, SARS-CoV, and
775 MERS-CoV viral load dynamics, duration of viral shedding, and infectiousness: a
776 systematic review and meta-analysis. The Lancet Microbe. 2021;2(1).
777 33. Graham KE, Loeb SK, Wolfe MK, Catoe D, Sinnott-Armstrong N, Kim S, et al. SARS-
778 CoV-2 RNA in Wastewater Settled Solids Is Associated with COVID-19 Cases in a Large
779 Urban Sewershed. Environ Sci Technol. 2021;55(1).
780 34. Gundy PM, Gerba CP, Pepper IL. Survival of Coronaviruses in Water and Wastewater.
781 Food Environ Virol. 2009;1(1).
782 35. Karthikeyan S, Ronquillo N, Belda-Ferre P, Alvarado D, Javidi T, Longhurst CA, et al.
783 High-Throughput Wastewater SARS-CoV-2 Detection Enables Forecasting of Community
784 Infection Dynamics in San Diego County. mSystems. 2021;6(2).
785 36. Galloway SE, Paul P, MacCannell DR, Johansson MA, Brooks JT, MacNeil A, et al.
786 Emergence of SARS-CoV-2 B.1.1.7 Lineage — United States, December 29, 2020–
787 January 12, 2021. MMWR Morb Mortal Wkly Rep. 2021;70(3).
788 37. Horby P, Huntley C, Davies N, Edmunds J, Ferguson N, Medley G, et al. NERVTAG note

on B.1.1.7 severity. Sage. 2021;
38. Washington NL, White S, Schiabor Barrett KM, Cirulli ET, Bolze A, Lu JT. S gene dropout patterns in SARS-CoV-2 tests suggest spread of the H69del/V70del mutation in the US. medRxiv. 2020.
39. Banks S. Column: Have half of L.A. County residents had COVID-19? It depends whose estimate you trust. Los Angeles Times. 2021 Mar 5;
40. Belin T, Bertozzi A, Chaudhary N, Graves T, Guterman J, Jarashow C, et al. Projections of Hospital-based Healthcare Demand due to COVID-19 in Los Angeles County. Los Angeles; 2021 Mar.